Cement & Concrete Composites 32 (2010) 291–299

Contents lists available at ScienceDirect

Cement & Concrete Composites

journal homepage: www.elsevier.com/locate/cemconcomp

Concrete porosimetry: Aspects of feasibility, reliability and economy

P. Stroeven *, J. Hu, D.A. Koleva

Faculty of Civil Engineering and Geosciences, Delft University of Technology, Stevinweg 1, 2628 CN Delft, The Netherlands

ARTICLE INFO

Article history:
Received in revised form 9 September 2009
Accepted 27 January 2010
Available online 2 February 2010

Keywords:
Cementitious materials
Connectivity
Image analysis
Opening operator
Pore size distribution

ABSTRACT

The opening operator of mathematical morphology is applied to section images in this paper for the assessment of pore characteristics, such as the size distribution, and critical pore size, in cement pastes. Moreover, the mean free spacing parameter is demonstrated as reflecting pore depercolation during cement maturation. This approach is compared with other popular methods for serving this purpose, encompassing the experimental technique of mercury intrusion porosimetry (MIP), Wood's metal intrusion porosimetry (WMIP), the conventional method of image analysis by area histogram and a direct 3D approach by a simulation model. The comparison study reveals that the opening distribution technique is superior in terms of feasibility, reliability and economy; realistic and relevant structural information on pore space in cement pastes is obtained. Nevertheless, star volume measurements applied to section images are referred to as an interesting alternative to the proposed method. The proper characterization of pore size distribution, and assessment of critical pore size, and delineation of percolated porosity zones are of significant importance to permeability prediction of cementitious materials and thereby to durability studies of the materials.

1. Introduction

Porosity and pore structure are among the most significant features of material microstructure that affect permeability and durability of cementitious materials. Therefore, proper characterization of pore structure would be crucial for modelling of permeability and for reliably estimating durability performance of the material. Porosity, pore connectivity and the so-called size distribution of pores (SDP) are generally used for this purpose. Pore size distribution can be determined indirectly by experimental techniques, such as mercury intrusion porosimetry (MIP) [1,2], or directly by way of quantitative image analysis observations [3–6]. The obvious drawback of experimental approaches is the necessity to make assumptions about pore geometry that lack microscopic evidence. In contrast, image analysis of two-dimensional (2D) sections of cement paste specimens provides a promising alternative for characterizing pore structure.

Pore space in hydrated cementitious materials can be seen as an interconnected structure of high complexity and tortuosity. The developments of techniques for image processing and quantitative image analysis have rendered possible direct observations and quantitative characterization of pore structure in cementitious materials. In doing so, numbers, areas, sizes and perimeter lengths can be assessed of the pore features observed on 2D section images. A conventional way to derive pore size distribution from section image analysis is the so-called area histogram, i.e., the pore features revealed on section image are classified according to their areas, whereupon the pore size distribution curve is obtained by plotting area fraction of porosity versus *equivalent pore diameter* (d), usually converted from $A = \pi d^2/4$, in which A stands for area of pore feature. Considering each pore area as individual feature, Lange et al. [3] directly measured the area-based cumulative pore size distribution curve, and found this to have a shape similar to that obtained by MIP, however, with a scale difference of about three orders of magnitude. Yet, as emphasized by Scrivener [5], and visualized by numerical models of the hydrated cement microstructure (e.g. [7,8]), pore structure is a complex interconnected network of irregular shape. It is therefore inappropriate to consider profiles of pore features (areas) as individual objects; hence, pore size distribution assessment by the area histogram method is basically incorrect. Moreover, even in the simplest case of dispersed mono-size spheres, is the section size distribution (or its average value) not related to size in 3D.

This contribution will therefore briefly describe a readily available and more reliable alternative provided by the so-called opening operation method. The method is unfortunately still quite obscure, although not completely unknown in our field [9,10]. Its use is promoted in this paper because of favourable scores as to feasibility, reliability and economy. Moreover, the method was recently applied to plain and reinforced concrete and mortar specimens for evaluation of micro-structural changes (both at interfaces and in the bulk cementitious matrix) in correlation with electrochemical phenomena [11,12]. Mathematical

* Corresponding author. Tel.: +31 15 278 4035; fax: +31 15 278 5767.
E-mail address: p.stroeven@tudelft.nl (P. Stroeven).

0958-9465/$ - see front matter © 2010 Elsevier Ltd. All rights reserved.
doi:10.1016/j.cemconcomp.2010.01.007

morphology techniques are based on measuring the changes produced when a binary image (reflecting the phase of interest) is transformed. The simplest mathematical morphology transformations are erosion, dilation, opening and closing. For a detailed description, see Serra [13].

Relevant to this work, the approach is *illustrated* by way of application to section images of concrete specimens. Since experimental work is not the prime subject of this contribution, details on concrete casting, conditioning, etc. are not hereby discussed (for details, see [14]). The presented experimental data are dealing with application of the *opening* distribution technique for characterization of porosity and the pore size distribution at the hydration age of 460 days of two differently conditioned but otherwise identical concrete specimens. One is a control specimen (tap water used for casting and conditioning), whereas the other was conditioned in NaCl (5% NaCl used as an external environment, i.e., chloride penetration was relevant for the total test period of 460 days).

As a readily available alternative, applicable to experimental as well as computer simulated settings, section images can be subjected at random points to so-called star volume measurements by 2D stars consisting of regularly or randomly spaced lineal segments. These unbroken linear line segments extend unobstructed to the pore perimeter. This will be discussed later.

The favourable characteristics of the proposed method are emphasized by mutually comparing with results, taken from representative sources in the open literature, obtained with conventional MIP, Wood's metal intrusion porosimetry (WMIP), area histogram method, and serial section 3D reconstruction. WMIP is a modified experimental technique similar to MIP, but employing Wood's metal as alternative of mercury for intrusion. Finally, characterization of porosity connectivity in concrete is briefly discussed on the basis of a simple example in which the stereological 3D operator mean free spacing is applied to sections.

In summary, it can be stated that the proposed method for porosimetry scores high as to feasibility, since no specialized equipment or extensive expertise would be required. Software is readily available and cheap, so the approach is economic. The reliable information on pore structure of cementitious materials that is obtained can be used for models to predict permeability of cementitious materials. To substantiate this latter statement, it can be mentioned that the proposed method is already proven to result in reliable (and reproducible) data on micro-structural properties of reinforced cement-based materials, supported by characterization of bulk matrix properties through electrochemical measurements. For example, porosity, pore size and pore interconnectivity of a bulk mortar matrix, which can be related to permeability and electrical properties, were correlated with electrical resistivity, derived from Electrochemical Impedance Spectroscopy [11]. Therefore it is strongly believed that insight into durability aspects of cementitious materials will be promoted by following the indicated procedure.

Other experimental techniques for porosimetry have been developed such as low temperature calorimetry (thermoporometry), adsorption/desorption isotherms [15], and X-ray microtomography [16]. Such techniques definitely resort under the more sophisticated approaches, whereas this paper concentrates on more commonly used relatively low-budget approaches to porosimetry, additionally asking only limited expertise. No attention is given either to probabilistic modelling, despite the claim to offer potentially more promising routes than provided by physical modelling that constitute the hard core of this paper [17,18]. However, concrete technologists will feel more familiar with physical modelling, because it can offer a more "realistic" representation of reality.

2. Conventional approaches to assessing pore characteristics

2.1. Mercury intrusion porosimetry (MIP)

It has been customary for quite some years to evaluate pore size distribution in cementitious materials by using MIP, despite the fact that drying of the specimens in the preparation procedure will exert significant effects on pore space. Based on the mercury intrusion data, the well-known Washburn equation [1,2] is thereupon applied to estimate the diameter of supposedly cylindrical pores intruded at each pressuring step. The Washburn model invokes two distinct assumptions as to the pores: (1) they are cylindrical and (2) they are accessible from the outer surface of the specimen. Of course, pore characteristics are supposed to represent those in the material used in practice. However, it has become increasingly apparent that the intrinsic pores in hydrated cement systems fail to conform to the requirements of the model [3]; pores are clearly not cylindrical, instead, most of their boundaries are obviously convoluted.

Wang and Diamond [19] have been evaluating pore shapes in cement pastes by quantitative image analysis (QIA). Very irregular and elongated shapes were determined by means of standard form factors. Furthermore, they found pore profiles to exhibit appreciably fractal nature by applying a standard progressive dilation technique. These findings demonstrate convincingly that the Washburn equation based on MIP data departs enormously from reality (as revealed by QIA). Most pores in this approach are two orders of magnitude smaller than they actually are. However, these effects appear even less important than due to violations of the accessibility condition.

The Washburn equation renders possible calculating the pressure required to fill a cylindrical pore of a given cross-sectional diameter with mercury, provided the pore is directly accessible to the mercury. This issue of accessibility to mercury appears to be at the root of the failure of MIP to provide realistic pore size distributions. The accessibility issue does not arise because individual pores may have ink-bottle shapes, as occasionally stated in the literature [4], but is far more fundamental than that. It arises from but a small proportion of the pores in hydrated cement specimens being directly connected to the exterior surface of the specimen that is subjected to the pressurized mercury. Nearly all of the pores are in the interior of the specimen, and most of them can be reached by mercury only through a long percolation chain of intermediate pores of varying sizes and shapes; the method is therefore referred to as an invasion percolation experiment [20]. This problem is explicitly explained and illustrated by Diamond [1].

Diamond [1] evaluated the deficiencies of MIP technique by comparing the SDP results obtained by MIP and by image analysis on 28 days old paste with w/c ratio of 0.4. The author reported that almost all of the pores obtained by image analysis were smaller than the MIP threshold diameter of the cement paste. Fig. 1a [1] presents a comparison between the two techniques for a cement paste containing air voids (deliberately designed for the experiment). It is clear that MIP data includes the air void volume as part of the measured porosity, but *disguises* the air void space by not intruding the air voids until the threshold diameter pressure is reached. Conversely, the image analysis technique, as a direct observation of the pore space, shows the air void space at appropriate diameters and, therefore, reveals a more realistic picture of the actual pore size distribution in cementitious materials. The aforementioned deficiencies of MIP technique have been extensively discussed and at least accepted by part of the cement researchers; among them, QIA of specimen sections is drawing rising interest as a more reliable alternative for pore structure analysis in cementitious materials. A combined use of MIP and QIA can also be

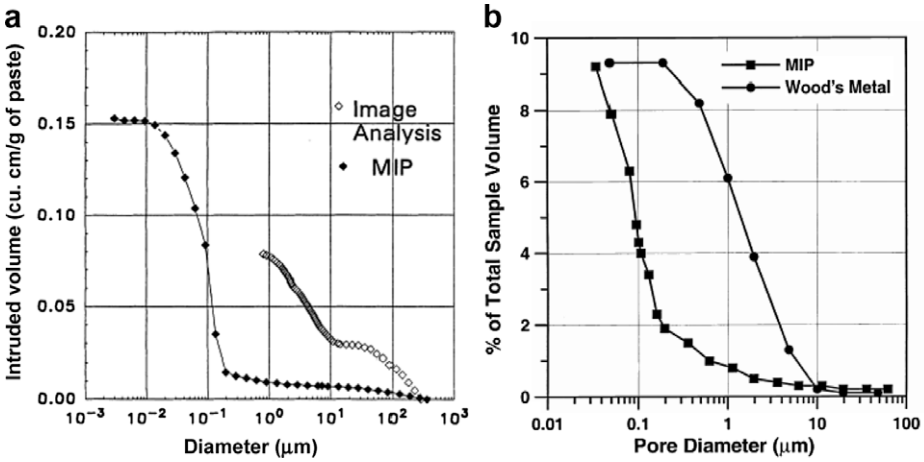

Fig. 1. (a) Comparison of MIP and QIA pore size distribution plots for 28 days old cement paste ($w/c = 0.4$) containing air voids (after Diamond [1]). (b) Comparison of pore size distributions results obtained by WMIP and MIP, respectively, for the aforementioned mortar but at the age of 14 days ($w/c = 0.4$) (after Willis et al. [4]).

pursued as stated by Roels et al. [20] "to determine main wetting and main drainage curves and to get a better insight, not only in pore volume distribution, but also in pore geometry and connectivity".

2.2. Image-based characterization by Wood's metal intrusion (WMIP)

Due to the aforementioned limitations of the MIP technique, some researchers replaced Wood's metal for mercury as the intruding liquid. The molten Wood's metal solidifies within the pore structure of the samples. This additionally allows for application of scanning electronic microscopy (SEM) and QIA to specimen sections. Scrivener and Nemati [21] employed Wood's metal for visualizing percolation of pore space in the interfacial transition zone (ITZ) in concretes, and found direct evidence of disproportionately higher pore connectivity, which should have direct impact on transport properties. Recent computer simulation studies by SPACE reveal a similar phenomenon, as will be discussed later on (e.g., Fig. 9). Willis et al. [4] investigated pore structure in an experimental approach also employing WMIP. It was found that molten Wood's metal has a contact angle on hydrated cement that is similar to that of mercury, and that its pressure versus volume intrusion curve into a mortar was essentially identical to that of mercury under the same conditions. However, with Wood's metal, the pressure applied can be released at any given level, so that after cooling down the location of the solidified Wood's metal within the specimen can be determined. The pore size distribution in the cement mortar was assessed thereupon by QIA. Fig. 1 provides results obtained by application of conventional MIP and of QIA to sections of the Wood's metal intruded mortar specimens. A practical observation, to which we will refer later, is that the intrinsic non-air void pores, revealed by the solidified Wood's metal, are mostly in the size range between 1 and 10 μm. Obviously, MIP data present incorrect information on pore size distribution, since pore size is derived on the basis of the diameter of the access throat through which the mercury has to penetrate the material to reach internal pores. As a result of this so-called ink-bottle effect, the MIP pore size distribution curve is shifted towards smaller size range by two or three orders of magnitude. The SDP information obtained by QIA and presented in Fig. 1 is based on the aforementioned area histogram approach. Although far more realistic SDP information is obtained by WMIP technique than by conventional MIP, the area histogram method that is used here is still restricted by the 2D character of pore features in sections. This was argued already in the introduction, and we will later come back to this issue. Nevertheless, it can be stated that although area fraction in isotropic structures can directly be associated through a stereological relationship with 3D volume fraction information, the 2D section size distribution cannot offers unbiased information as to 3D size. This straightforward approach by area classification belongs to individual granulometric analysis [13]. The quality of SPD characterization can be improved by the opening distribution technique that will be described in what follows. As discussed elsewhere in this paper, QIA can be considered a proper alternative as well.

2.3. Porosimetry on 3D-reconstructed model cement paste

Ye et al. [7] developed a software package for three-dimensional (3D) reconstruction from serial sections of pore space in the matured state. This renders possible directly deriving 3D information on pore size distribution in the model material that is generated by the HYMOSTRUC3D discrete element computer simulation package. This system is based on a so-called random sequential addition (RSA) algorithm for particle packing in the fresh state that seriously limits the scope of application possibilities as will be discussed later. The pore structure in simulated cement paste is interpreted as the free space between expanding cement particles during the hydration process. The volume fraction of pores accessible to imaginary testing spheres of radius r_i, denoted as $\rho(r_i)$, can be computed by gradually filling testing spheres into pore space that are thereupon subjected to compaction to yield a densely packed mono-size sphere filling. This is repeated for a wide range of pore diameters, r. The cumulative pore size distribution curve is obtained by directly plotting $\rho(r)$ versus r. It can be expected that $\rho(r)$ is a monotonically decreasing function of r. The pore size distribution curve can be represented by the derivative of the cumulative curve. For a detailed description of this simulation approach and an example, see Ye et al. [7,8].

This time-consuming approach provides a rather straightforward 3D measurement of volume-based pore size distribution. Still, it should be noted that the assessed pore volume at a certain value of r constitutes but a lower bound estimate. However, when the minimum radius and the interval between radii of testing spheres are small enough at the specified resolution, this method can provide reasonable results [7]. In addition, the calculation results also depend on the starting point of the testing process, an effect of which the impact is larger the radius of the test spheres. Only a randomly selected starting point and

averaging over different trials could solve this problem. This would make the approach even more time-consuming, however. For model cement pastes with w/c ratios of 0.6 and 0.3, Ye's data revealed critical pore sizes of about 3 μm and 1.5 μm, respectively, at 4 days of hydration (corresponding to a degree of hydration of 0.64).

2.4. SDP from sections by means of star volume application

It should be emphasized that for continuous phases consisting of a complex and convoluted system of tunnels and cavities, as in case of pore space in cementitious materials, conventional measurements of volume and surface area are of little practical use in describing 'size' [13]. Other examples of this type of phase include the alveolar air spaces in lung, and the pore space in porous rocks such as sandstone. An available and feasible definition of size for this type of phase – including pores – is the so-called *star volume*. This is defined as the average of the volume (area in 2D) that can be seen unobstructed in starred directions from a random point within the phase of interest [13], as illustrated in Fig. 2. Take the pore space as set X, the set Y_x (light grey area) includes all points $y \in X$ that can be seen directly from point x. When x is arbitrary, the zone of direct vision (Y_x) varies from point to point. The star allows the definition of a mean volume of the connected pores. The star volume v^* at point x can be estimated in an unbiased way on the basis of the unbroken linear intercept lengths l_i for random directions in the section plane (as shown in Fig. 2b) by

$$v^* = \frac{\pi}{3}\overline{l_i^3} \tag{1}$$

The mean star volume of the pore space is the average of v^* for a large number of random points and random directions chosen uniformly among all 3D orientations. In addition, the histogram of measured star values represents the actual pore size distribution (SDP) in 3D space. For non-isotropic structures, a set of isotropic uniform random (IUR) *sections* should be prepared. For additional practical information, see Gundersen and Jensen [22]. Of course, this method allows deriving pore size distribution in a far more efficient and economic way than in the 3D reconstruction approach can be realized. Moreover, it can be employed in experiments as well as in computer simulation approaches, and can be considered a reasonable alternative for the opening distribution technique discussed in the next section.

3. Assessment of pore characteristics by opening operation

3.1. Opening distribution technique

Clustering of objects in space can be studied by volume fraction measurements (of the phase of interest) after applying a *dilation* operation with structural elements of increasing size [23]. In a similar type of approach, pore size distribution in cement paste can be determined by means of volume fraction measurements after an *opening* operation is accomplished on pore space with structural elements of increasing size [5,6]. These are examples of granulometric distribution functions in mathematical morphology.

Two main categories of the so-called granulometric distribution methods in sections can be distinguished: measurement by individual analysis or by morphological opening. Individual granulometric analysis is well-known: the size of each pore feature in the binary image is measured. Then they are classified according to their size to yield the size distribution function. In contrast to individual granulometric analysis, the morphological *opening* distribution offers according to Delfiner [24] a suitable approach to analyzing a complex, interconnected structural phase like pores, since it can be used independently of the nature of the phase of interest (pore space in this study). He further states that the *erosion* operator alone could be applied to measure size distribution of isolated elements (like particles). On the basis of mathematical morphology transformations, various distributions reflecting pore phase can be obtained by using a sequence of similarly shaped structuring elements (a square in this study) of increasing size. The *opening distribution* curve of pore space is obtained by plotting the pore area fraction after an opening operation (as illustrated in Fig. 3) versus the linear dimension of the structuring element. This gives a type of *size classification* in the case of an interconnected structure (Fig. 4), in contrast to single features as in the case of individual granulometric analysis (e.g., area histogram). The measure by opening distribution technique is a 2D analogue (with 3D information) of the type of size distribution obtained by gas or methanol absorption or by low temperature calorimetry [5]. It offers, in very economic way consistent and reliable information on characteristics of pore space, SDP inclusive.

3.2. Determination of critical pore size

The definition of critical pore size (denoted as l_c) can be found in the literature [2]. It is conceived as the diameter of the pore that completes the first interconnected pore pathway in a network

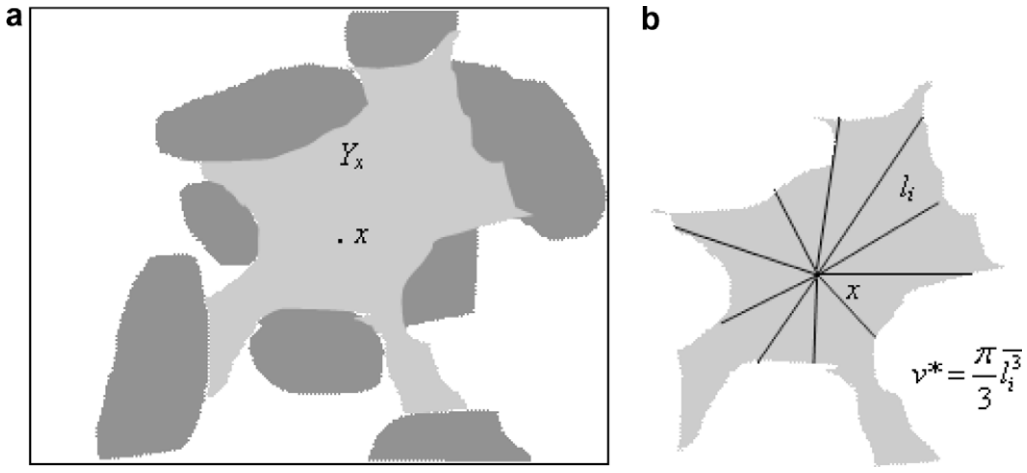

Fig. 2. 2D schematic drawing of the star of the pores, defined as the volume of the light grey zone v^* averaged for all points x in the pore space. The distribution (histogram) of the star volume as x spans the pore space gives insight into the pore size distribution.

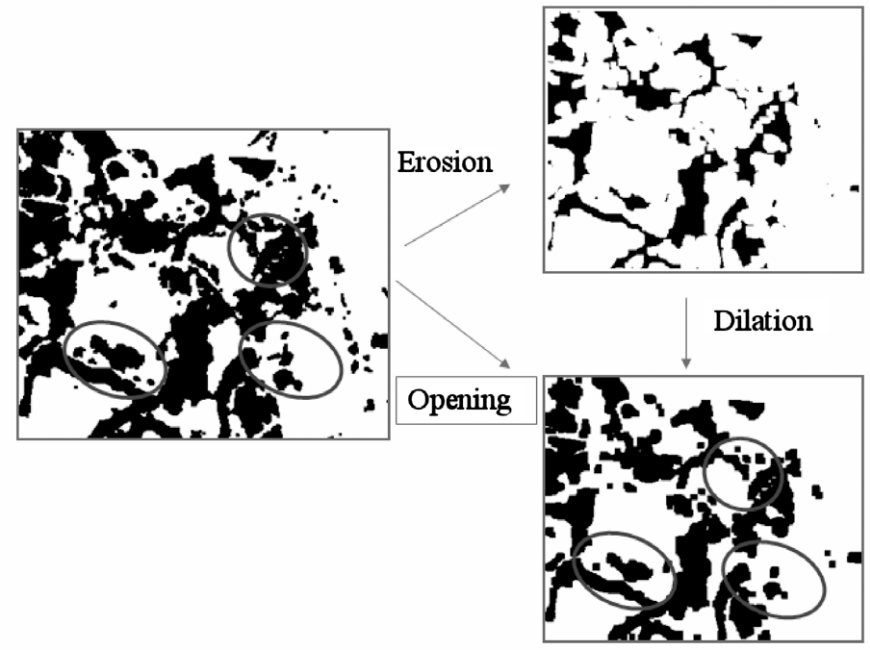

Fig. 3. Illustration of an opening operation, i.e., an erosion operation followed by a dilation operation with the same structuring element. Please note the structural changes in the circled regions after application of the opening operation.

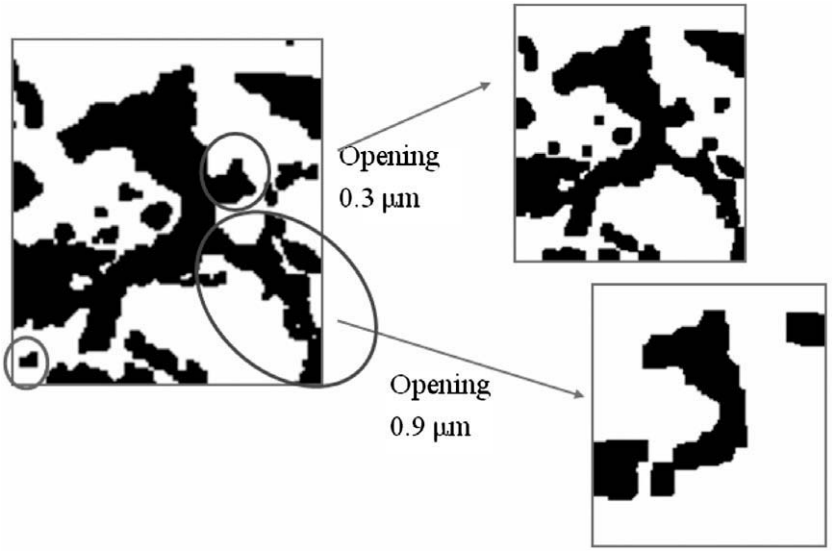

Fig. 4. Opening distribution by structuring elements of increasing sizes gives a sort of size classification. By an opening with square structuring element of 0.9 μm, the lower circled region is removed; hence this local branch area is contributing to the size range < 0.9 μm.

developed by a procedure of sequentially adding pores of diminishing size to this network. It is generally accepted that the smaller the critical pore size, the finer the pore structure. The critical pore size is a unique transport length scale of major significance for permeability properties. Katz and Thompson [2] supported the conjecture that mercury injection is of percolation geometry and considered the characteristic length l_c as corresponding to the percolation threshold. So, it can be experimentally assessed by MIP. A typical mercury injection curve (as shown in [2]), reflecting the volume percentage of mercury intruded as a function of the applied pressure, is S-shaped; after a gradual increase under rising pressure, a rapid rise in volume percentage of mercury intrusion occurs at a certain pressure, whereupon gradually a plateau value is reached. This stage of rapid rise is interpreted as the moment when the intruded mercury has formed the first connected cluster spanning the sample. The inflection point of the rapidly rising portion of the curve can be seen as the percolation threshold. Similarly, the critical pore size l_c can be associated with the inflection point of the opening distribution curve, and with the peak of the derivative curve of the opening distribution curve.

3.3. Influence of image resolution

The optical magnification required for visualization of the material microstructure at the level of the researcher's interest defines both the micro-structural level displayed by the field, and the geometric structure of the representative volume element (RVE). Hence, optical resolution and observed level of the microstructure

are intimately connected: higher densities of geometric parameters will be observed under higher optical resolution. It is necessary to strike a balance between a representative area element revealing sufficiently large pore section, and a satisfactory resolution for detection of small capillary pores.

The first two authors [6] studied the influence of resolution on the accuracy of the critical pore size determined by the opening distribution. It was found that a resolution of 0.488 μm/pixel fails to differentiate pore structures between 7 and 28 days of hydration. Although at the highest magnification (2000×) trivial as well as subtle changes of the pore structure were revealed, resolutions of 0.293 and 0.146 μm/pixel result in similar values of the critical pore size. It has been proven that the fraction of pores between 0.1 and 10 μm is highly correlated with cement permeability (with a correlation coefficient of 0.953) [25]. Therefore, it is reasonable to study cement permeability with image analysis techniques, as long as a satisfactory resolution of about 0.20 μm per pixel is ensured.

4. Illustrative results and discussion

4.1. Pore size distribution

4.1.1. SDP obtained by opening distribution technique

Overall measurement of porosity P is fairly straightforward as the average pore area fraction measured on 2D sections is an unbiased estimate of the volume fraction of pore space [18]. Fig. 5a and b depicts representative micrographs of the investigated concretes. Fig. 5c and d presents the derived structural information after an opening distribution technique. It is hereby worthwhile mentioning that the image analysis was performed on a representative number of images for each specimen (at least 35 locations (section images) per sample of 20×20 mm, thus providing statistical accuracy). Additionally, the image analysis excludes the aggregate fraction and considers only the bulk cement paste (as illustrated by the rectangular marked regions in Fig. 5a and b). For more details on the application of the technique to reinforced cement-based materials, see [9,12,14,26].

Fig. 5c presents the opening distribution curve for the tested bulk concretes (two specimens in each group) and the cumulative pore size distribution curves for each group of concretes, D and N, respectively. Total porosity equals the value of the opening distribution curve at zero size of structuring element, leading to 7.97% (D specimen) and 3.29% (N specimen), respectively (concrete age 460 days). Sodium chloride (as involved in the conditioning of specimen N) normally accelerates the hydration process [27,28] therefore a lower porosity in the N specimen can be expected. The critical pore size l_c is determined as shown in Fig. 5d. The value of l_c is 0.634 μm in the N specimen, lower than the 0.951 μm in the D specimen. The critical pore size will decrease with hydration time. Further, the higher w/c ratio, the larger will be the critical pore size. It is not possible to convert the opening distribution directly into a 3D representation of the pore size distribution, but it would be useful to have a measure for expressing differences between pore structures in cementitious materials. Moreover, comparison with 3D calculations (see [7]) revealed good correspondence between the curve patterns and the size ranges. This demonstrates that the SPD obtained by means of the opening distribution offers realistic 3D structural information of pore space in cementitious materials.

Fig. 6 provides a comparison between pore size measurements by means of opening distribution and by the conventional area histogram. Since the structuring element used in the opening distribution technique is a square, the pore size (x-axis) in Fig. 6 is converted by $l = \sqrt{A}$. Alternatively, $l = \sqrt{2A}$ could have been

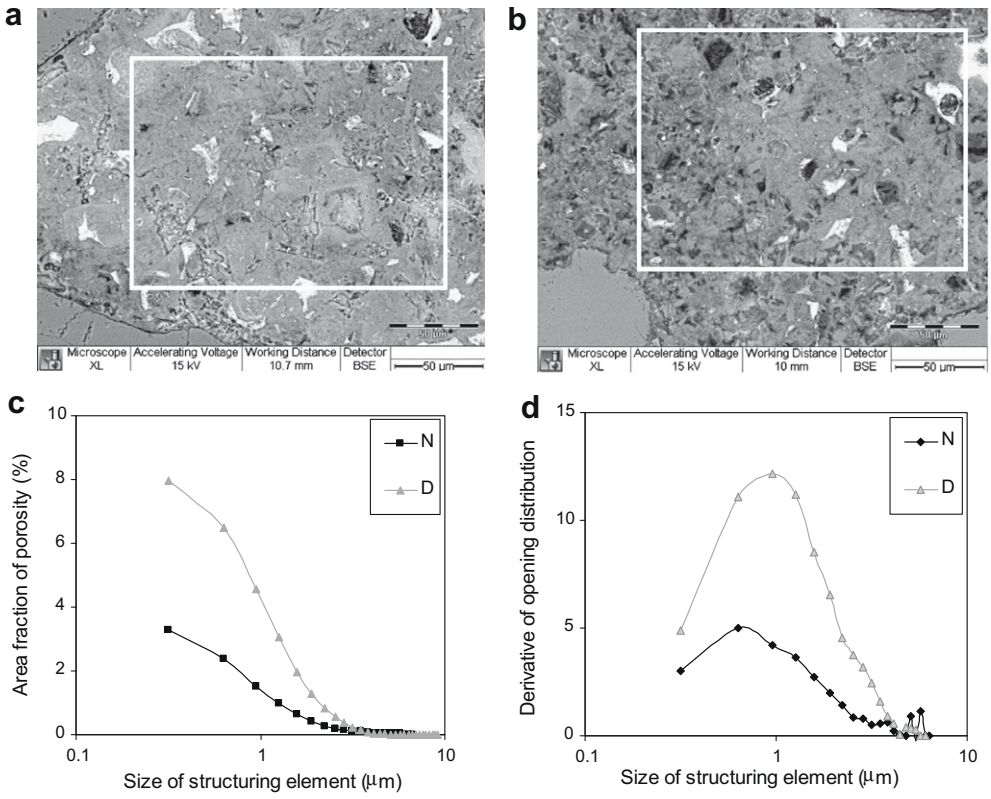

Fig. 5. (a and b) SEM micrographs of concrete specimen N and D respectively (magnification of 500×), depicting the area for image analysis (marked area). (c) Pore size distribution (opening distribution) curves for concrete with w/c ratio of 0.6 at 460 days of hydration. (d) Determination of critical pore size from derivatives of pore size distribution curves; peak point corresponds to the inflection point on the pore size distribution curve.

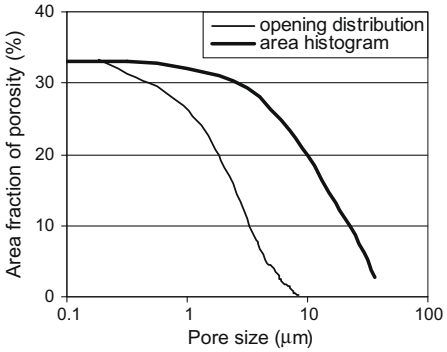

Fig. 6. Pore size distribution curves obtained by application of the opening distribution technique and by area histogram, for a cement paste with *w*/*c* ratio of 0.5 at 3 days hydration.

employed, however, this does not change the conclusions that can be drawn. Obviously, the shape and size range covered by the SDP curve as obtained by opening distribution resembles the results of WMIP presented in Fig. 1b to a better extent than defined by the area histogram. This confirms that the conventional area histogram is not suitable for characterizing size distribution of such a highly interconnected structure like pore space in cementitious systems. This was already stipulated in the introduction. In contrast, a mathematical morphology technique like opening distribution can provide far more realistic structural information of pore space.

4.1.2. Number-based pore size distribution

Two histograms can be drawn from the fundamental sorting on the basis of pore volume, i.e., volume-based pore size distribution (volume fraction of pores in a specific size range) and number-based distribution (number of pore features in a specific size range). The general definition of pore size distribution, as in the cases of opening distribution and MIP data, refers to the first catalogue. So, the area histogram constitutes a 2D analogue of the volume-based distribution with respect to pore features on the section image. Note that both volume- and number-based histograms represent the same raw data, but they focus on different aspects of the pore size distribution. Number-based distribution assigns equal statistical 'weight' to each pore feature regardless of its area. The number-based pore size distribution of 2D pore features on section images can be assigned 3D character when corrected according to a method introduced by DeHoff and Rhines [29]. Fig. 7 provides a comparison between the 2D number-based pore size distribution obtained in the morphological opening approach and the corresponding 3D distribution, revealing that the

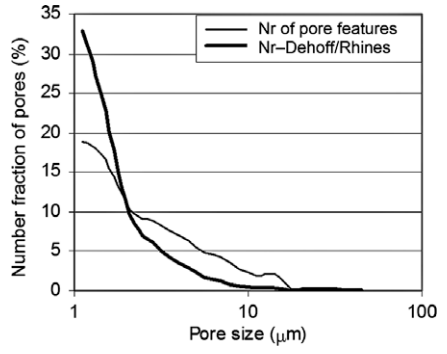

Fig. 7. Number-based pore size distribution (frequency, in %) derived from number of pore features on section image assessed by morphological opening transformation.

direct 2D representation of number-based histogram significantly underestimates the number fraction (i.e., the number-based portion) of pores smaller than 2 μm.

4.2. Porosity connectivity

Section images of cement paste and concrete specimens cannot provide direct information on pore connectivity. However, pore structure evolution during maturation of cementitious materials can be considered a geometrical–statistical (=stereological) process. The solid phase (cement particles plus hydration products) gradually develops into a connected network, which contributes significantly to the material strength. In contrast, the pore space changes to a de-percolated structure in the matured material as a result of the continuous decline in porosity and in pore connectivity during the hydration process. Spacing parameters defined in stereological theory [18], characterize spatial dispersion of the solid phase and of the pores, providing insight into the connectivity of pore space in matured cementitious materials. From this point of view, the first two authors [30] discussed the depercolation threshold porosity for *model cement pastes* with different water cement ratios and cement finesses levels on the basis of mean free spacing between elements of the solid phase. The involved model cements were generated with the SPACE system [31] that *realistically* simulates particle packing (mutual spacing, configuration of grains) and cement hydration in concrete composites, since based on concurrent (i.e., particle interaction) algorithms [32].

This requires making a comment on the *type* of computer simulation systems used for structural development of cementitious materials. Random sequential addition (RSA) procedures are generally used in concrete technology for simulating the fresh state of cement particle packing (the initial situation before cement hydration). In contrast, SPACE is a so-called concurrent algorithm-based system (CAS) [33]. When interested in the assessment of composition aspects of the materials such as bulk porosity, RSA systems will suffice. However, when focusing on the mutual arrangement of pores so on pore clustering or pore percolation, CAS should be employed, since it provides a far more reliable basis for progress. It has been demonstrated that configuration sensitive information on pore space (e.g., pore connectivity) can only be generated in a reliable way by CAS, like SPACE or newest HADES system [34]. The pore structure in CAS simulated maturing cement paste was found easier to de-percolate (corresponding to lower pore connectivity) although total porosity was slightly higher than in RSA-based model cements at the same hydration age. This confirms that correct information on *pore topology* demands realistic modelling of particle configuration in the fresh state that is underlying the hydration simulation.

In this contribution, relevant to concrete technology, the heterogeneity in material structure (with respect to pore connectivity) will be briefly discussed for a *model concrete*. Fig. 8 shows the mean free spacing plotted against the distance to the rigid aggregate surface for a model paste at the fresh state of cement particle packing and for the 100-h matured paste. Particle size ranges from 1 to 45 μm. At the initial packing state, the measured mean free spacing in the bulk cement (Fig. 8a) is about 3.5 μm, in line with the stereological estimate on the basis of *w*/*c* ratio:

$$\lambda = 4\frac{1-V_V}{S_V} = 4\frac{1-V_V}{S_G\rho_{cem}V_V} = 4\frac{1-0.51}{340\times 3.15\times 10^3\times 0.51}\,\mathrm{m} = 3.56\times 10^{-6}\,\mathrm{m} \quad (2)$$

where S_V is the surface area of cement particles per unit of test volume, S_G is the Blain fineness (i.e., specific surface area per unit mass of the cement particles, in m^2/kg), ρ_{cem} is the density of fresh

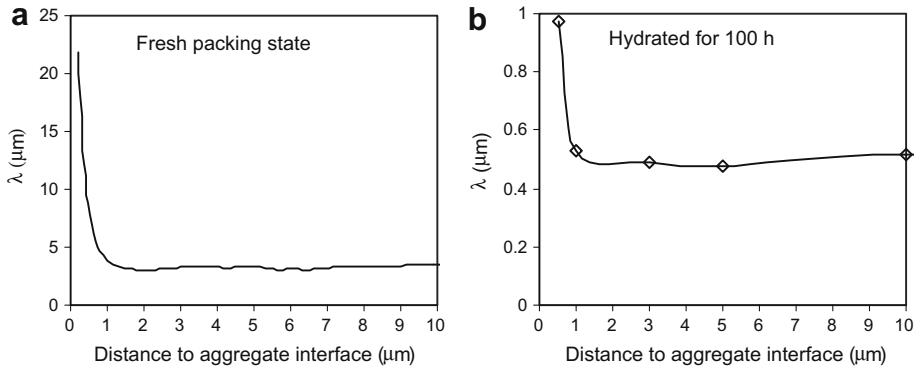

Fig. 8. Mean free spacing plotted again distance to the aggregate interface in the fresh packed model concrete with $w/c = 0.3$, cement specific surface area of 340 m^2/kg (a), and in the hardened concrete hydrated for 100 h (b).

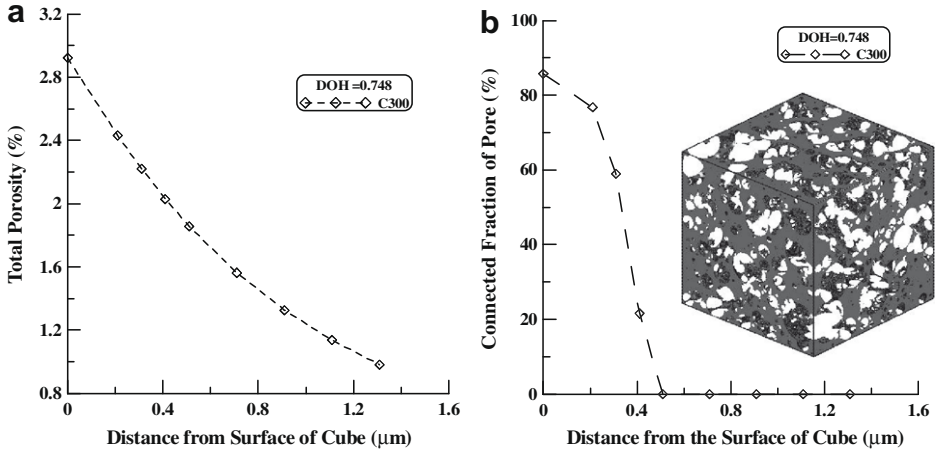

Fig. 9. Total porosity (a) and capillary pore connectivity (b, with visualization) inside the interfacial transition zone for density (ITZ). The involved water cement ratio is 0.3, and the degree of hydration is 0.748 (ultimate degree of hydration).

cement (3.15×10^3 kg/m^3), V_V is the volume fraction of cement particles (0.51 corresponding to w/c of 0.3). The spacing parameter is significantly reduced in the matured concrete (Fig. 8b). The present authors have demonstrated that depercolation phenomenon and the relevant threshold porosity are associated with the morphological evolution of the pore space (characterized by mean free spacing). The mean free spacing will reduce significantly during the first period of hydration, and then gradually reaches a stable and low value at the depercolation threshold porosity [29]. Hence, this spacing parameter gives insight into pore connectivity. Fig. 8b reveals that the bulk cement past in the matured concrete is disconnected, while in the immediate vicinity (up to 1.5 μm from the aggregate surface) the pore space is still partly connected. Chen et al. [34] calculated the pore connectivity in a straightforward way (making use of Ye's 3D reconstruction algorithm), according to the conventional definition of connectivity as connected fraction of porosity, for a model concrete with similar technical parameters ($w/c = 0.3$, Blaine fineness of 300 m^2/kg) at the ultimate degree of hydration. This study revealed that the connected porosity is restricted to a very narrow zone immediately neighbouring (within 0.5 μm distance, in Fig. 9) the aggregate surface as part of the conventional ITZ for material density (because of the roughly 50% reduced particle size range in the model cement, the corresponding ITZ's thickness for density would be about 25 μm). The results obtained on the basis of mean free spacing are in good agreement with the direct calculation of connected porosity, confirming that the spacing parameter reflects the geometrical aspects of the hydration process.

5. Summary and conclusions

This contribution presents a critical evaluation in terms of feasibility, reliability and economy of different methods applicable for characterizing pore size distribution of cementitious materials, among which are the conventional experimental techniques as mercury intrusion porosimetry (MIP), and a modified experimental approach with Wood's metal (WMIP), the conventional area histogram of pore features displayed in section images, and the opening distribution technique. It is argued that quantitative image analysis, when combined with mathematical morphology operations (specifically, opening), will provide relatively realistic structural information of the pore space in cementitious materials. Part of quantitative image analysis could be application of the star volume to random positions in the image plane. This is an economic alternative for the morphological opening operation, also yielding unbiased 3D information on pore size distribution.

Critical pore size can be derived from the opening distribution curve. Values of critical pore size (also referred to as threshold diameter in literature) and of porosity are useful indexes of pore structure for mutually comparing between cement pastes or mortars. Total porosity varies with w/c ratio and hydration time in a similar way as the critical pore size. The critical pore size seems to be a valid comparative parameter, related to permeability and ion diffusion in cement systems. The proper characterization of pore structure is expected to provide important information for modelling permeability of cementitious materials; hence, it is highly relevant to studies of durability aspects of the materials.

Cement hydration and structural developments in cementitious materials are processes governed by geometrical laws. The stereological spacing parameter (mean free spacing) can be used to characterize the structural evolution and to estimate pore connectivity in cementitious materials during the hydration process.

References

[1] Diamond S. Mercury porosimetry: an inappropriate method for the measurement of pore size distributions in cement-based materials. Cem Concr Res 2000;30(10):1517–25.
[2] Katz AJ, Thompson AH. Quantitative prediction of permeability in porous rock. Phys Rev B 1986;34(11):8179–81.
[3] Lange DA, Jennings HM, Shah SP. Image analysis techniques for characterization of pore structure of cement-based materials. Cem Concr Res 1994;24(5):841–53.
[4] Willis KL, Abell AB, Lange DA. Image-based characterization of cement pore structure using Wood's metal intrusion. Cem Concr Res 1998;28(12):1695–705.
[5] Scrivener KL. The use of backscattered electron microscopy and image analysis to study the porosity of cement paste. In: Roberts LR, Skalny JP, editors. Proceedings of material research society symposium 137. Boston: Material Research Society; 1989. p. 129–40.
[6] Hu J, Stroeven P. Application of image analysis to assessing critical pore size for permeability prediction on cement paste. Image Anal Stereol 2003;22(2):97–103. <http://www.wise-t.com/ias>.
[7] Ye G, van Breugel K, Fraaij ALA. Three-dimensional microstructure analysis of numerically simulated cementitious materials. Cem Concr Res 2003;33:215–22.
[8] Ye G, Hu J, van Breugel K, Stroeven P. Characterization of the development of microstructure and porosity of cement-based materials by numerical simulation and ESEM image analysis. Mater Struct 2002;35:603–13.
[9] Dilks A, Graham SC. Prediction of permeability behaviour of reservoir rocks on acid treatment by means of the morphological opening transformation. Extended Abstracts In: Proc 4th Eur symp for stereology. Göteborg: Chalmers University of Technology; 1985. p. 96.
[10] Thovert JF, Salles S, Adler PM. Computerized characterization of the geometry of real porous media: their discretization, analysis and interpretation. J Microsc 1993;170(1):65–79.
[11] Koleva DA, van Breugel K, de Wit JHW, van Westing E, Copuroglu O, Veleva L, et al. Correlation of microstructure, electrical properties and electro-chemical phenomena in reinforced mortar. Breakdown to multi-phase interface structures. Part I: microstructural observations and electrical properties. Mater Charact 2008;59(3):290–300.
[12] Koleva DA, de Wit JHW, van Breugel K, Veleva LP, van Westing E, Copuroglu O, et al. Correlation of microstructure, electrical properties and electrochemical phenomena in reinforced mortar. Breakdown to multi-phase interface structures. Part II: pore network, electrical properties and electrochemical response. Mater Charact 2008;59(6):801–15.
[13] Serra J. Image analysis and mathematical morphology. London: Academic Press; 1982.
[14] Koleva DA, Copuroglu O, van Breugel K, Ye G, de Wit JHW. Electrical resistivity and microstructural properties of concrete materials in conditions of current flow. Cem Concr Compos 2008;30(8):731–44.
[15] Brun M, Lallemand A, Quinson JF, Eyraud C. A new method for simultaneous determination of the size and shape of pores: the thermoporometry. Thermochim Acta 1977;21:59–88.
[16] Bentz DP, Mizell S, Satterfield S, Devaney J, George W, Ketcham P, et al. The visible cement data set. J Res Natl Inst Stand Technol 2002;107(2):137–48.
[17] Dequiedt AS, Coster M, Chermant J-L, Jeulin D. Towards a model of concrete mesostructure. Cem Concr Compos 2001;23:289–97.
[18] Underwood EE. Quantitative stereology. New Jersey: Addison-Wesley Publishing Company; 1968.
[19] Wang Y, Diamond S. An approach to quantitative image analysis for cement pastes. In: Diamond S, Mindess S, Glasser FP, Roberts LW, Skalny JP, Wakeley LD, editors. Microstructure of cement based systems/bonding and interfaces in cementitious materials. Proceedings of Material Research Society 370. Pittsburgh: Material Research Society; 1995. p. 23–32.
[20] Roels S, Elsen J, Carmeliet J, Hens H. Characterization of pore structure by combining mercury porosimetry and micrography. Mater Struct 2001;34(2):76–82.
[21] Scrivener KL, Nemati KM. The percolation of pore space in the cement paste/aggregate interfacial zone of concrete. Cem Concr Res 1995;26:35–40.
[22] Gundersen HJG, Jensen EB. Stereological estimation of the volume-weighted mean volume of arbitrary particles observed on random sections. J Microsc 1985;138:127–42.
[23] Jeulin D. Random texture models for material structures. Stat Comput 2000;10:121–32.
[24] Delfiner P. A generalization of the concept of size. J Microsc 1971;95:203–16.
[25] Bágel L, Živica V. Relationship between pore structure and permeability of mortars. Cem Concr Res 1997;27:1225–35.
[26] Koleva DA, van Breugel K, de Wit JHW, van Westing E, Boshkov N, Fraaij A. Electrochemical behaviour, microstructural analysis and morphological observations in reinforced mortar subjected to chloride ingress. J Electrochem Soc 2007;154(3):E45–56.
[27] Díaz B, Nóvoa XR, Pérez MC. Study of the chloride diffusion in mortar: a new method of determining diffusion coefficients based on impedance measurements. Cem Concr Compos 2006;28:237–45.
[28] Suryavanshi AK, Scantlebury JD, Lyon SB. Pore size distribution of OPC and SRPC mortars in presence of chlorides. Cem Concr Res 1995;25:980–8.
[29] DeHoff RT, Rhines FN. Quantitative microscopy. New York: McGraw-Hill; 1968.
[30] Hu J, Stroeven P. Depercolation threshold of porosity in model cement; approach by morphological evolution during hydration. Cem Concr Compos 2005;27(1):19–25.
[31] Stroeven M. Discrete numerical model for the structural assessment of composite materials. Ph.D. Thesis. Delft: Delft University Press; 1999.
[32] Williams SR, Philipse AP. Random packings of spheres and spherocylinders simulated by mechanical contraction. Phys Rev E 2003;67(051301):1–9.
[33] Stroeven P, Guo Z. Modern routes to explore concrete's complex pore space. Image Anal Stereol 2006;25:75–86. <http://www.wise-t.com/ias>.
[34] Chen H, Stroeven P, Ye G, Stroeven M. Influence of boundary conditions on pore percolation in model cement paste. Key Eng Mater 2006;303:486–92.